

Substituent Control of Hydrogen Bonding in Palladium(II)–Pyrazole Complexes

Douglas B. Grotjahn,^{*,†} Sang Van,[†] David Combs,^{†,‡} Daniel A. Lev,[†] Christian Schneider,^{†,§} Christopher D. Incarvito,^{||} Kim-Chung Lam,^{||} Gene Rossi,^{||,§} Arnold L. Rheingold,^{||} Marc Rideout,^{†,§} Christoph Meyer,^{†,§} Genaro Hernandez,^{†,§} and Lupe Mejorado^{†,§}

Department of Chemistry, 5500 Campanile Drive, San Diego State University, San Diego, California 92182-1030, and Department of Chemistry and Biochemistry, University of Delaware, Newark, Delaware 19716

Received October 12, 2002

Inter- and intramolecular hydrogen bonding of an N–H group in pyrazole complexes was studied using ligands with two different groups at pyrazole C-3 and C-5. At C-5, groups such as methyl, *i*-propyl, phenyl, or *tert*-butyl were present. At C-3, side chains L–CH₂– and L–CH₂CH₂– (L = thioether or phosphine) ensured formation of chelates to a *cis*-dichloropalladium(II) fragment through side-chain atom L and the pyrazole nitrogen closest to the side chain. The significance of the ligands is that by placing a ligating side chain on a ring carbon (C-3), rather than on a ring nitrogen, the ring nitrogen not bound to the metal and its attached proton are available for hydrogen bonding. As desired, seven chelate complexes examined by X-ray diffraction all showed intramolecular hydrogen bonding between the pyrazole N–H and a chloride ligand in the *cis* position. In addition, however, intermolecular hydrogen bonding could be controlled by the substituent at C-5: complexes with either a methyl at C-5 or no substituent there showed significant intermolecular hydrogen bonding interactions, which were completely avoided by placing a *tert*-butyl group at C-5. The acidity of two complexes in acetonitrile solutions was estimated to be closer to that of pyridinium ion than those of imidazolium or triethylammonium ions.

Introduction

A major focus of ongoing work in our laboratories is the study of hydrogen bonding or proton donation in transition metal complexes,^{1–3} and how such features can improve catalysis.¹ Metalloenzymes are an inspiration for this work.⁴ For example, in carboxypeptidase,⁵ it is thought that the combined effects (cooperativity) of a Zn(II) ion and nearby Brønsted–Lowry acids and bases are responsible for facili-

tating the addition of a water molecule to a carboxylic acid amide, accelerating amide hydrolysis by a factor of more than 10¹¹.^{6,7}

Bioorganic and bioinorganic chemists have studied cooperativity between metal ions and organic functional groups such as phenol,⁸ imidazole or imidazolium,⁹ and alkylamine or -ammonium moieties,^{10,11} the relevant acidic forms of which are characterized by p*K*_a values in the range 7–10. Organometallic examples of cooperativity or bifunctional catalysis have emerged in the past 10 years. Here, a transition metal hydride and an N–H or O–H^{12–17} group act in concert,

* To whom correspondence should be addressed. E-mail: grotjahn@chemistry.sdsu.edu.

[†] San Diego State University.

[‡] Current address: Trilink Biotechnologies, San Diego, CA.

[§] Undergraduate research participant.

^{||} University of Delaware.

(1) Grotjahn, D. B.; Incarvito, C. D.; Rheingold, A. L. *Angew. Chem., Int. Ed.* **2001**, *40*, 3884–3887.

(2) Grotjahn, D. B.; Combs, D.; Van, S.; Aguirre, G.; Ortega, F. *Inorg. Chem.* **2000**, *39*, 2080–2086.

(3) Grotjahn, D. B.; Van, S.; Combs, D.; Kassel, W. S.; Rheingold, A. L. *J. Inorg. Biochem.* **2001**, *85*, 61–65.

(4) Sadler, P. J. *Metal Sites in Proteins and Models*; Springer: Heidelberg, 1997; Vol. 89.

(5) Creighton, T. E. *Proteins: Structures and Molecular Properties*, 2nd ed.; W. H. Freeman: New York, 1993.

(6) Bryant, R. A. R.; Hansen, D. E. *J. Am. Chem. Soc.* **1996**, *118*, 5498–5499.

(7) Radzicka, A.; Wolfenden, R. *J. Am. Chem. Soc.* **1996**, *118*, 6105–6109.

(8) Schepartz, A.; Breslow, R. *J. Am. Chem. Soc.* **1987**, *109*, 1814–1826.

(9) Breslow, R.; Berger, D.; Huang, D. *J. Am. Chem. Soc.* **1990**, *112*, 3687–3688.

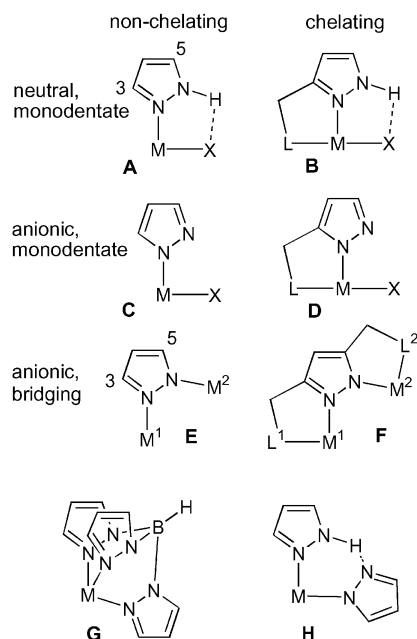
(10) Kövári, E.; Krämer, R. *J. Am. Chem. Soc.* **1996**, *118*, 12704–12709.

(11) Wall, M.; Linkletter, B.; Williams, D.; Lebus, A.-M.; Hynes, R. C.; Chin, J. *J. Am. Chem. Soc.* **1999**, *121*, 4710–4711.

(12) Noyori, R.; Hashiguchi, S. *Acc. Chem. Res.* **1997**, *30*, 97–102.

(13) Palmer, M. J.; Wills, M. *Tetrahedron: Asymmetry* **1999**, *10*, 2045–2061.

Chart 1. Pyrazole Coordination Modes



delivering two hydrogens in the reduction of polar functional groups such as aldehydes, ketones, or imines. In the metal hydride systems studied, the N–H or O–H group is electronically coupled to the metal center bearing the hydride. Related work on hydrogen bonding interactions in organometallic complexes also exists.^{18–21} We propose to extend the study of such systems, using other ligands, particularly heterocycles.

The pyrazole heterocycle forms metal complexes^{22–26} in a wide variety of coordination modes, some of which are schematically illustrated in Chart 1. Bridging, anionic pyrazolates are very common (structures **E** and **F**),²⁶ as are the versatile tris(pyrazolyl)borates (**G**) and related systems.^{27,28} Hundreds of poly(pyrazolyl)borate complexes (**G**) are known, because of the robust nature of the ligand and the ability to make derivatives of different steric and electronic properties.^{27,28} Further, bridging pyrazolates (**E** and **F**) are useful

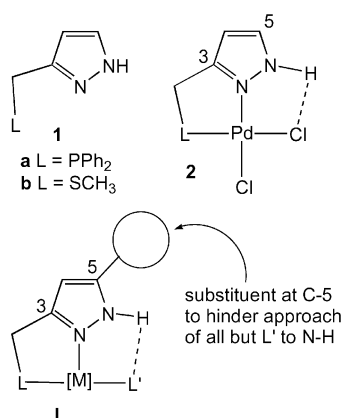
in studying bimetallic reactivity and cooperativity and electronic communication between metals, to name a few properties of interest in coordination, bioinorganic, and organometallic chemistry.^{23–25,29–44}

However, we have been very interested in the rarer coordination mode shown in **A–D**, because complexes of this type are expected to show an interplay between the metal center and the N–H moiety (**A** and **B**) or between the metal center and the uncoordinated, basic N (**C** and **D**). Examples of ligands to which a metal-coordinated pyrazole can intramolecularly donate a hydrogen bond include halide, hydroxide, or peroxo species.^{2,45–56} Fascinating structures such as **H** are also known.^{53,57,58} As for the acidity of metal-coordinated pyrazoles, the measured pK_a of pyrazole complexes of $Cr^{III}(NH_3)_5$ and $Co^{III}(NH_3)_5$, and $Ru^{III}(NH_3)_5$,^{59,60}

- (14) Yamakawa, M.; Ito, H.; Noyori, R. *J. Am. Chem. Soc.* **2000**, *122*, 1466–1478.
- (15) Abdur-Rashid, K.; Faatz, M.; Lough, A. J.; Morris, R. H. *J. Am. Chem. Soc.* **2001**, *123*, 7473–7474.
- (16) Noyori, R.; Ohkuma, T. *Angew. Chem., Int. Ed.* **2001**, *40*, 40–73.
- (17) Casey, C. P.; Singer, S. W.; Powell, D. R.; Hayashi, R. K.; Kavana, M. *J. Am. Chem. Soc.* **2001**, *123*, 1090–1100.
- (18) Patel, B. P.; Crabtree, R. H. *J. Am. Chem. Soc.* **1996**, *118*, 8, 13105–13106.
- (19) Yao, W.; Crabtree, R. H. *Inorg. Chem.* **1996**, *35*, 3007–3011.
- (20) Chu, H. S.; Lau, C. P.; Wong, K. Y.; Wong, W. T. *Organometallics* **1998**, *17*, 2768–2777.
- (21) Lee, D.-H.; Patel, B. P.; Clot, E.; Eisenstein, O.; Crabtree, R. H. *J. Chem. Soc., Chem. Commun.* **1999**, 297–298.
- (22) Elguero, J. Pyrazoles. In *Comprehensive Heterocyclic Chemistry*; Shinkai, I., Ed.; Pergamon: Oxford, 1996; Vol. 3, pp 1–75.
- (23) Sadimenko, A. P.; Basson, S. S. *Coord. Chem. Rev.* **1996**, *147*, 247–297.
- (24) Garnovskii, A. D.; Sadimenko, A. P. *Adv. Heterocycl. Chem.* **1999**, *72*, 1–77.
- (25) Mukherjee, R. *Coord. Chem. Rev.* **2000**, *203*, 151–218.
- (26) la Monica, G.; Ardizzioia, G. A. *Prog. Inorg. Chem.* **1997**, *46*, 151–238.
- (27) Trofimenko, S. *Chem. Rev.* **1993**, *93*, 943–980.
- (28) Kitajima, N.; Tolman, W. B. *Prog. Inorg. Chem.* **1995**, *43*, 419–531.

- (29) Mani, F. *Coord. Chem. Rev.* **1992**, *120*, 325–359.
- (30) Bode, R. H.; Bol, J. E.; Driessen, W. L.; Hulsbergen, F. B.; Reedijk, J.; Spek, A. L. *Inorg. Chem.* **1999**, *38*, 1239–1243.
- (31) Yu, Z.; Wittbrodt, J. M.; Heeg, M. J.; Schlegel, H. B.; Winter, C. H. *J. Am. Chem. Soc.* **2000**, *122*, 9338–9339.
- (32) Cámpora, J.; López, J. A.; Maya, C. M.; Palma, P.; Carmona, E. *Organometallics* **2000**, *19*, 2707–2715.
- (33) Carmona, D.; Ferrer, J.; Arilla, J. M.; Reyes, J.; Lahoz, F. J.; Elipse, S.; Modrego, F. J.; Oro, L. A. *Organometallics* **2000**, *19*, 798–808.
- (34) Catalano, V. J.; Craig, T. J. *Polyhedron* **2000**, *19*, 475–485.
- (35) Bohle, D. S.; Sagan, E. S. *Eur. J. Inorg. Chem.* **2000**, 1609–1616.
- (36) Südfeld, M.; Sheldrick, W. S. *Inorg. Chim. Acta* **2000**, *304*, 78–86.
- (37) Paneque, M.; Sirol, S.; Trujillo, M.; Carmona, E.; Gutiérrez-Puebla, E.; Monge, M. A.; Ruiz, C.; Malbosc, F.; Serra-Le Berre, C.; Kalck, P.; Etienne, M.; Daran, J. C. *Chem. Eur. J.* **2001**, *7*, 3868–3879.
- (38) Meyer, F.; Jacobi, A.; Zsolnai, L. *Chem. Ber./Recl.* **1997**, *130*, 1441–1447.
- (39) Meyer, F.; Ruschewitz, U.; Schober, P.; Antelmann, B.; Zsolnai, L. *J. Chem. Soc., Dalton Trans.* **1998**, 1181–1186.
- (40) Konrad, M.; Meyer, F.; Heinze, K.; Zsolnai, L. *J. Chem. Soc., Dalton Trans.* **1998**, 199–205.
- (41) Meyer, F.; Hyla-Kryspin, I.; Kaifer, E.; Kircher, P. *Eur. J. Inorg. Chem.* **2000**, 771–781.
- (42) Meyer, F.; Pritzkow, H. *Angew. Chem., Int. Ed.* **2000**, *39*, 2112–2115.
- (43) Schade, C.; Schleyer, P. v. R. *Adv. Organomet. Chem.* **1987**, *27*, 159–278.
- (44) Chou, J.-L.; Jong-Pyng Chyn, J.-P.; Urbach, F. L.; Gervasio, D. L. *Polyhedron* **2000**, *19*, 2215–2223.
- (45) Mighell, A. D.; Reimann, C. W.; Santoro, A. *Acta Crystallogr. B* **1969**, *B25*, 595–599.
- (46) Reimann, C. W. *J. Chem. Soc., Chem. Commun.* **1969**, 145–146.
- (47) Johnson, D. A.; Deese, W. C.; Cordes, A. W. *Acta Crystallogr., Sect. B* **1981**, *B37*, 2220–2223.
- (48) Deese, W. C.; Johnson, D. A. *J. Organomet. Chem.* **1982**, *232*, 325–333.
- (49) Taqui Khan, M. M.; Khan, N. H.; Kureshy, R. I.; Venkatasubramanian, K. *Polyhedron* **1992**, *11*, 431–441.
- (50) Osawa, M.; Singh, U. P.; Tanaka, M.; Moro-oka, Y.; Kitajima, N. *J. Chem. Soc., Chem. Commun.* **1993**, 310–311.
- (51) Kitajima, N.; Osawa, M.; Tamura, N.; Moro-oka, Y.; Hirano, T.; Hirobe, M.; Nagano, T. *Inorg. Chem.* **1993**, *32*, 1879–1880.
- (52) Esteruelas, M. A.; García, M. P.; Martín, M.; Nürnberg, O.; Oro, L. A.; Werner, H. *J. Organomet. Chem.* **1994**, *466*, 249–257.
- (53) García, M. P.; Esteruelas, M. A.; Martín, M.; Oro, L. A. *J. Organomet. Chem.* **1994**, *467*, 151–159.
- (54) Warda, S. A.; Friebe, C. J.; S.; Plesch, G.; Bláhova, M. *Acta Crystallogr., Sect. C* **1997**, *C53*, 50–54.
- (55) Komatsuzaki, H.; Ickawa, S.; Hikichi, S.; Akita, M.; Moro-oka, Y. *Inorg. Chem.* **1998**, *37*, 3652–3656.
- (56) Esteruelas, M. A.; Oliván, M.; Oñate, E.; Ruiz, N.; Tajada, M. A. *Organometallics* **1999**, *18*, 2953–2960.
- (57) Carmona, D.; Oro, L. A.; Lamata, M. P.; Elguero, J.; del Carmen Apreda, M.; Foces-Foces, C.; Cano, F. H. *Angew. Chem., Int. Ed. Engl.* **1986**, *25*, 1114–1115.
- (58) Carmona, D.; Ferrer, J.; Oro, L. A.; Apreda, M. C.; Foces-Foces, C.; Cano, F. H.; Elguero, J.; Jimeno, M. L. *J. Chem. Soc., Dalton Trans.* **1990**, 1463–1476.
- (59) Johnson, C. R.; Henderson, W. W.; Shepherd, R. E. *Inorg. Chem.* **1984**, *23*, 2754–2763.

Scheme 1



are in the range 5.98–7.21, similar to that of protonated imidazole, but much lower than the pK_a of pyrazole itself (14.2).⁶¹ One report appearing in 1998, as we began our work, showed the potential difficulties of maintaining structures such as **A–D** under basic conditions: Cu(II) complexes of type **A** undergo deprotonation and dimerization (forming bridging structures similar to **E**) rather than catalyze phosphate ester hydrolysis.⁶²

In our pursuit of structures **A** or **B** in which an N–H bond is retained, we have reported preparation of pyrazole ligands **1a** and **1b** (Scheme 1) featuring a soft thioether or phosphine group.² (For clarity in this paper, in all cases where two tautomeric forms of a pyrazole are possible and probable, e.g., **1**, only one form will be shown.) In the crystal structures of Pd(II) species of type **B** (e.g., **2**), it was obvious that a lack of steric hindrance at the pyrazole N–H allowed multiple hydrogen bonding interactions, both the desired intramolecular one shown, as well as undesired intermolecular ones. Therefore, we have begun to investigate new pyrazole ligands as schematically shown in **I** (Scheme 1), where the bulk of a substituent at C-5 is expected to control approach of all but cis-oriented ligand L' to the pyrazole N–H. The work reported here uses our recently developed synthesis of pyrazole ligands⁶³ to place even a *tert*-butyl or adamantyl group at C-5. Herein, the crystal structures of seven PdCl₂ complexes show that changing the group at C-5 allows control of the structure of the complexes and their intermolecular hydrogen bonding. In addition, because so little is known about the acidity of coordinated pyrazoles,^{59,60} we have examined some of the Pd(II) species herein. These results are expected to make pyrazoles and pyrazolates more versatile ligands in catalysis, supramolecular chemistry, and other fields.

Experimental Section

General. Bis(acetonitrile)palladium(II) dichloride was either purchased or prepared in a manner similar to that reported for the benzonitrile analogue.⁶⁴ Ligands were made as previously re-

ported.⁶³ Solvents for manipulations of phosphines were deoxygenated by bubbling nitrogen through them. Reactions were performed under nitrogen using a combination of Schlenk and inert-atmosphere glovebox techniques, and workups were done in air unless otherwise specified.

NMR spectra were recorded at 200 or 500 MHz with Varian spectrometers at 30 °C. ¹H and ¹³C NMR chemical shifts are reported in ppm downfield from tetramethylsilane and referenced to residual solvent resonances [¹H NMR: 7.27 for CHCl₃ in CDCl₃ and 2.50 for CHD₂SOCD₃ in (CD₃)₂SO. ¹³C NMR: 77.23 for CDCl₃ and 39.51 for CD₃SOCD₃], where ¹H NMR signals are given followed by multiplicity, coupling constants *J* in hertz, integration in parentheses. For complex coupling patterns, the first coupling constant listed corresponds to the first splitting listed, e.g., for (dt, *J* = 3.2, 7.9, 1 H), the doublet exhibits the 3.2-Hz coupling constant. ³¹P{¹H} NMR chemical shifts were referenced to external 85% H₃PO₄ (aq).

IR spectra were obtained in KBr disks or in solutions held in NaCl cells using an FT-IR spectrophotometer (either Nicolet Nexus 670 or Perkin-Elmer 1600 series). Elemental analyses were performed at NuMega Resonance Labs (San Diego).

Complex 2c. To PdCl₂(NCCH₃)₂ (0.151 g, 0.58 mmol) was added deoxygenated methanol (3 mL). To the resulting orange solution was added a solution of phosphine-pyrazole **1c** (0.171 g, 0.61 mmol) in methanol (3 mL). After the reaction mixture stirred for 16 h at room temperature, a yellow precipitate formed. The reaction slurry was filtered, and the yellow-orange solid was washed with CH₂Cl₂ (1 × 10 mL). The resulting yellow solid was placed under high vacuum to yield **2c** (0.96 g, 0.21 mmol, 36%) as a powder. Slow evaporation of dichloromethane from a dilute solution of **2c** in a mixture of methanol/dichloromethane (1:1) afforded crystals suitable for X-ray analysis. ¹H NMR [(CD₃)₂SO, 500 MHz] δ 12.65 (s, 1 H, NH), 7.90–7.85 (m, 4 H, ortho H), 7.66–7.64 (m, 2 H, para H), 7.59–7.55 (m, 4 H, meta H), 6.30 (s, 1 H, H4), 3.97 (d, 2 H, *J* = 13.0 Hz, CH₂P), 2.29 ppm (s, 3 H, pzCH₃). ¹³C-{¹H} NMR [(CD₃)₂SO, 125.7 MHz] δ 152.5 (d, *J* = 8.7 Hz), 144.7, 133.0 (d, *J* = 11.1 Hz), 132.1, 129.0 (d, *J* = 11.6 Hz), 127.6 (d, *J* = 55.7 Hz, C_{ipso}), 104.1 (d, *J* = 12.8 Hz), 28.8 (d, *J* = 32.3 Hz), 11.0 ppm. ³¹P{¹H} NMR [(CD₃)₂SO, 80.95 MHz] δ 46.81 ppm. IR (KBr) 3222, 3121, 2916, 1558, 1437, 1391, 1278, 1183, 1103, 1051 cm⁻¹. Elemental analysis calcd (%) for C₁₇H₁₇Cl₂N₂PPd (457.63): C, 44.62; H, 3.74; N, 6.12. Found: C, 44.23; H, 3.62; N, 5.84.

Complex 2d. The phosphine ligand **1d** (59.3 mg, 0.184 mmol) in CH₂Cl₂ was allowed to stir with PdCl₂(CH₃CN)₂ (49.2 mg, 0.190 mmol). Within 15 min the mixture became a clear yellow solution. After 20 h, the solvent was removed in vacuo. To the residue was added hexanes, giving an orange solid (71.7 mg, 72%). ¹H NMR (CDCl₃, 500 MHz) δ 11.51 (s, 1 H, NH), 7.90 (ddd, *J* = 1.1, 8.2, 13.1 Hz, 4 H, ortho H), 7.59 (tt, *J* = 1.1, 7.5 Hz, 2 H, para H), 7.48–7.52 (m, 4 H, meta H), 6.23 (d, *J* = 2.2 Hz, 1 H, H4), 5.27 (s, 1 H, 0.5 CH₂Cl₂), 3.65 (d, *J* = 12.1 Hz, 2 H, CH₂P), 1.33 ppm [s, 9 H, C(CH₃)₃]. ¹³C{¹H} and DEPT NMR (CDCl₃, 50.3 MHz) δ 156.8 (C), 152.4 (d, *J* = 6.7 Hz, C), 133.3 (d, *J* = 11.2 Hz, CH), 132.4 (d, *J* = 3.2 Hz, CH), 129.3 (d, *J* = 12.0 Hz, CH), 127.7 (d, *J* = 56.5 Hz, C_{ipso}), 101.6 (d, *J* = 12.6 Hz, CH), 53.6 (CH₂Cl₂), 31.9 [C(CH₃)₃], 31.1 (d, *J* = 32 Hz, CH₂P), 29.75 [C(CH₃)₃] ppm. ³¹P{¹H} NMR (CDCl₃, 80.95 MHz) δ 45.1 ppm. IR (CH₂Cl₂, NaCl) 3312, 3047, 2973, 1548, 1438, 1208, 1105 cm⁻¹. Elemental analysis calcd (%) for C₂₀H₂₃Cl₂NPPd·0.5 CH₂Cl₂ (499.69 + 42.47): C, 45.42; H, 4.46; N, 5.17. Found: C, 45.91; H, 4.22; N, 5.36.

(64) Doyle, J. R.; Slade, P. E.; Jonassen, H. B. *Inorg. Synth.* **1960**, 6, 216–219.

(60) Winter, J. A.; Caruso, D.; Shepherd, R. A. *Inorg. Chem.* **1988**, 27, 1086–1089.

(61) Yagil, G. *Tetrahedron* **1967**, 23, 2855–2861.

(62) Deters, R.; Krämer, R. *Inorg. Chim. Acta* **1998**, 269, 117–124.

(63) Grotjahn, D. B.; Van, S.; Combs, D.; Lev, D.; Schneider, C.; Rideout, M.; Meyer, C.; Hernandez, G.; Mejorado, L. *J. Org. Chem.* **2002**, 67, 9200–9209.

Complex 2e. To a solution of thioether ligand **2e** (0.199 g, 1.08 mmol) in methanol (7 mL) under nitrogen atmosphere was added at room temperature $\text{PdCl}_2(\text{CH}_3\text{CN})_2$ (0.280 g, 1.08 mmol). After the reaction mixture stirred for 10 h, an orange-yellow precipitate had formed. The reaction mixture was filtered, and the solid was washed with cold methanol (1 mL). The solid residue was placed under vacuum to give **2e** (0.336 g, 0.930 mmol, 86%) as a yellow solid. Crystals suitable for X-ray analysis were grown from the diffusion of acetone into a solution of **2e** in $(\text{CD}_3)_2\text{SO}$. ^1H NMR [$(\text{CD}_3)_2\text{SO}$, 500 MHz] δ 12.29 (s, 1 H, NH), 6.37 (s, 1 H, H4), 4.28 (d, $J = 16.5$ Hz, 1 H, CHHS), 3.96 (d, $J = 16.5$ Hz, 1 H, CHHS), 2.59 (s, 3 H, SCH_3), 1.29 ppm [s, 9 H, $\text{C}(\text{CH}_3)_3$]. $^{13}\text{C}\{^1\text{H}\}$ NMR [$(\text{CD}_3)_2\text{SO}$, 125.7 MHz] δ 157.2, 155.0, 101.5, 35.3, 31.5, 29.2, 23.0 ppm. IR (KBr) 3366, 3125, 2964, 2924, 2864, 1611, 1546, 1450, 1360, 1214, 1054, 807, 706, 576 cm^{-1} . Elemental analysis calcd (%) for $\text{C}_9\text{H}_{16}\text{Cl}_2\text{N}_2\text{PdS}$ (361.61): C, 29.89; H, 4.46; N, 7.75. Found: C, 29.91; H, 4.35; N, 7.78.

Complex 2f. Ligand **2f** (50.0 mg, 0.157 mmol) and $\text{PdCl}_2(\text{CH}_3\text{CN})_2$ (40.6 mg, 0.157 mmol) were stirred with methanol for 5 h. The precipitate was filtered off. After drying under vacuum, **2f** (35.2 mg, 57%) remained. ^1H NMR (CDCl_3 , 500 MHz) δ 9.6 (br s, 1 H, NH), 7.37 (dd, $J = 2, 8$ Hz, 2 H, ortho H), 7.27 (dt, $J = 2, 7.5$ Hz, 2 H, meta H), 7.19 (tt, $J = 1.5, 7.5$ Hz, 1 H, para H), 6.01 (s, 1 H, H4), 4.16 (s, 2 H, CH_2S), 1.31 ppm [s, 9 H, $\text{C}(\text{CH}_3)_3$]. $^{13}\text{C}\{^1\text{H}\}$ NMR (CDCl_3 , 125.7 MHz) δ 155.9, 146.9, 136.4, 129.4, 128.8, 126.2, 100.9, 31.2, 31.1, 30.2 ppm. $^{13}\text{C}\{^1\text{H}\}$ NMR [$(\text{CD}_3)_2\text{SO}$, 125.7 MHz] δ 157.5, 155.1, 130.4, 130.3, 130.0, 129.1, 101.4, 37.6, 31.6, 29.2. IR (KBr) 3397 (s), 3122, 2969, 2867, 1544, 1467, 1401, 1283, 1214, 1050, 883, 833, 750, 677 cm^{-1} . Elemental analysis calcd (%) for $\text{C}_{14}\text{H}_{18}\text{Cl}_2\text{N}_2\text{PdS}$ (423.68): C, 39.69; H, 4.28; N, 6.61. Found: C, 39.27; H, 4.20; N, 6.61.

Complex 2g. To a solution of hydroxy-substituted ligand **2g** (0.066 g, 0.31 mmol) in methanol (5 mL) under nitrogen atmosphere was added at room temperature $\text{PdCl}_2(\text{CH}_3\text{CN})_2$ (0.080 g, 0.31 mmol). After stirring 15 h, the reaction mixture was concentrated and the residue recrystallized from diethyl ether and filtered. The solid was washed with ether (1 mL) and placed under vacuum to give **2g** (0.096 g, 0.25 mmol, 80%) as a yellow solid. Crystals suitable for X-ray analysis were grown from slow evaporation of a solution of **2g** in CDCl_3 . ^1H NMR [$(\text{CD}_3)_2\text{SO}$, 500 MHz] δ 12.22 (s, 1 H, NH), 6.34 (s, 1 H, H4), 5.22 (bs, 1H, OH), 4.19 (d, $J = 16.5$ Hz, 1 H, CHHS), 4.14 (d, $J = 16.5$ Hz, 1 H, CHHS), 3.85 (m, 2 H, $\text{SCH}_2\text{CH}_2\text{OH}$), 3.14 (m, 2 H, $\text{SCH}_2\text{CH}_2\text{OH}$), 1.29 ppm [s, 9 H, $\text{C}(\text{CH}_3)_3$]. $^{13}\text{C}\{^1\text{H}\}$ NMR [$(\text{CD}_3)_2\text{SO}$, 50.3 MHz] δ 157.4, 155.7, 101.4, 59.3, 41.8, 33.7, 31.5, 29.2 ppm. IR (KBr) 3522 (sharp), 3333 (broad), 3122, 2953, 2874, 1551, 1461, 1399, 1287, 197, 1129, 1056, 995, 809, 714 cm^{-1} . Elemental analysis calcd (%) for $\text{C}_{10}\text{H}_{18}\text{Cl}_2\text{N}_2\text{OPdS}$ (391.65): C, 30.67; H, 4.63; N, 7.15. Found: C, 30.78; H, 4.63; N, 7.38.

Complex 2h. To a solution of thioether ligand **2h** (0.0123 g, 0.0543 mmol) in methanol (2 mL) under nitrogen atmosphere was added at room temperature $\text{PdCl}_2(\text{CH}_3\text{CN})_2$ (0.0141 g, 0.0543 mmol). After stirring for 15 h, ether was added, but no precipitate formed. Hexanes (5 mL) was added to induce crystallization. The reaction mixture was filtered, and the solid was washed with cold hexanes (1 mL). The solid residue was placed under vacuum to give **2h** (0.0210 g, 0.0516 mmol, 95%) as a yellow solid. Crystals suitable for X-ray analysis were grown by slow evaporation of a solution of **2h** in CDCl_3 . ^1H NMR (CDCl_3 , 500 MHz) δ 10.96 (s, 1 H, NH), 6.19 (s, 1 H, H4), 3.99 (d, $J = 16.5$ Hz, 1 H, CHHS), 3.67 (d, $J = 16.5$ Hz, 1 H, CHHS), 1.60 [s, 9 H, $\text{C}(\text{CH}_3)_3$], 1.32 ppm [s, 9 H, $\text{C}(\text{CH}_3)_3$]. $^{13}\text{C}\{^1\text{H}\}$ (CDCl_3 , 125.7 MHz) δ 156.9, 155.2, 100.8, 55.1, 32.1, 31.1, 30.4, 29.9 ppm. IR (KBr) 3344, 3120,

2966, 2877, 1550, 1467, 1291, 1156, 1050, 805, 760, 649 cm^{-1} . Elemental analysis calcd (%) for $\text{C}_{12}\text{H}_{22}\text{Cl}_2\text{N}_2\text{PdS}$ (403.71): C, 35.70; H, 5.49; N, 6.94. Found: C, 35.84; H, 5.42; N, 6.81.

Complex 5d. Solid $\text{PdCl}_2(\text{CH}_3\text{CN})_2$ (135 mg, 0.52 mmol) was added to a stirred solution of phosphine **4d** (175 mg, 0.52 mmol) dissolved in methanol (10 mL). After stirring the solution for 2 h, solvent was removed on a rotary evaporator. The orange solid remaining was dissolved in a minimum amount of methylene chloride, and an equal volume of diethyl ether was added. The light yellow precipitate was filtered and rinsed with diethyl ether (2×10 mL), followed by pentane (10 mL). Product **5d** (215 mg, 0.42 mmol, 81%) was obtained as a yellow solid. X-ray quality crystals were obtained by recrystallization from methylene chloride with diethyl ether diffusion. ^1H NMR (CDCl_3 , 200 MHz) δ 12.74 (bs, 1 H, NH), 7.88–8.00 (m, 4 H, ortho H), 7.42–7.58 (m, 6 H, meta and para H), 5.95 (d, 1 H, $J = 2.4$ Hz, H4), 2.70–2.90 (m, 2 H), 2.28–2.40 (m, 2 H), 1.32 ppm [s, 9 H, $\text{C}(\text{CH}_3)_3$]. $^{31}\text{P}\{^1\text{H}\}$ NMR (CDCl_3 , 80.95 MHz) δ –6.30 ppm. $^{13}\text{C}\{^1\text{H}\}$ NMR (CDCl_3 , 50.3 MHz) δ 154.9, 147.6 (d, $J = 5$ Hz), 134.1 (d, $J = 10.6$ Hz), 132.1 (d, $J = 2.8$ Hz, C_{para}), 129.0 (d, $J = 11.8$ Hz), 127.7 (d, $J = 60.8$ Hz, C_{ipso}), 104.2, 29.7, 27.8, 20.2, 19.4 ppm. IR (KBr) 3165, 2964, 1560, 1545, 1477, 1459, 1436, 1400, 1369, 1290, 1267, 1218, 1159, 1100, 1053, 998, 852, 829, 810, 745, 708 cm^{-1} . Elemental analysis calcd (%) for $\text{C}_{21}\text{H}_{25}\text{Cl}_2\text{N}_2\text{PPd}$ (513.74): C, 49.10; H, 4.90; N, 5.45. Found: C, 49.38; H, 4.76; N, 5.49.

Complex 5e. Solid $\text{PdCl}_2(\text{CH}_3\text{CN})_2$ (385 mg, 1.49 mmol) was added to a stirred solution of thioether ligand **4e** (294 mg, 1.49 mmol) in methanol (10 mL). After the solution was stirred for 30 min, the orange precipitate formed was filtered, washed with methanol (2×5 mL), and air-dried. The product **5e** (402 mg, 1.07 mmol, 72%) was obtained as an orange solid. X-ray quality crystals were obtained by recrystallization from methanol. ^1H NMR [$(\text{CD}_3)_2\text{SO}$, 500 MHz] δ 12.19 (s, 1 H), 6.27 (d, 1 H, $^4J_{\text{HH}} = 2.5$ Hz), 3.56 (m, 1 H), 2.63 (t, 2 H, $^3J_{\text{HH}} = 5$ Hz), 2.59 (s, 3 H), 1.76 (m, 1 H), 1.26 [s, 9 H, $\text{C}(\text{CH}_3)_3$]. $^{13}\text{C}\{^1\text{H}\}$ NMR [$(\text{CD}_3)_2\text{SO}$, 125.7 MHz] δ 155.1, 146.9, 103.0, 31.2, 29.2, 28.9, 23.9, 21.3 ppm. IR (KBr) 3322, 2962, 1560, 1543, 1467, 1438, 1412, 1366, 1277, 1240, 1219, 1178, 1159, 1123, 1053, 1026, 1004, 974, 880, 808, 718 cm^{-1} . Elemental analysis calcd (%) for $\text{C}_{10}\text{H}_{18}\text{N}_2\text{S}$ (373.96): C, 31.97; H, 4.83; N, 7.46. Found: C, 31.87; H, 4.73; N, 7.43.

X-ray Crystallography. The crystal data and details of X-ray diffraction experiments are given in Tables 1 and 2. The diffraction data are uniquely consistent with the reported space groups and yielded chemically reasonable and computationally stable results of refinement. All structures were solved by direct methods, completed by subsequent difference Fourier syntheses, and refined by full-matrix least-squares procedures. All non-hydrogen atoms were refined with anisotropic displacement coefficients, and hydrogen atoms, with the exception of the pyrazolyl protons noted, were treated as idealized contributions. The positions of the pyrazolyl protons in **2c–g** and **5e** were determined from the electron difference map and refined with isotropic displacement coefficients, whereas in **2h** and **5d** they were calculated. All software and sources of the scattering factors are contained in the SHELXTL program libraries (G. Sheldrick, Siemens XRD, Madison, WI).

Results and Discussion

Synthesis. The number of pyrazole-containing ligands in which both ring nitrogens are unsubstituted and a side chain is attached at a ring carbon is rather small,^{38–40,44,62,65–71} probably because it is relatively difficult to make such systems. However, we recently reported a method to

Table 1. Collection Data for Crystal Structures of **2c**, **2d**, **2e**, and **2g**^a

	2c	2d	2e	2g
formula	C ₁₇ H ₁₇ Cl ₂ N ₂ PPd	C _{20.5} H ₂₄ Cl ₃ N ₂ PPd	C ₉ H ₁₆ Cl ₂ N ₂ PdS	C ₁₀ H ₁₈ Cl ₂ N ₂ OPdS
MW	457.60	542.14	361.60	391.62
cryst dimensions (mm ³)	0.30 × 0.15 × 0.15	0.20 × 0.20 × 0.15	0.40 × 0.40 × 0.30	0.10 × 0.05 × 0.05
cryst syst	monoclinic	monoclinic	orthorhombic	monoclinic
space group	<i>P</i> 2 ₁ / <i>c</i>	<i>C</i> 2/ <i>c</i>	<i>Pbca</i>	<i>P</i> 2 ₁ / <i>c</i>
<i>a</i> [Å]	11.5347(6)	19.8959(3)	12.0199(2)	11.7418(2)
<i>b</i> [Å]	13.0646(7)	9.7947(2)	10.4778(2)	10.3303(2)
<i>c</i> [Å]	12.1248(6)	23.9010(3)	21.4984(2)	11.8937(2)
α [deg]	90	90	90	90
β [deg]	98.1200(10)	105.2729(2)	90	93.8162(7)
γ [deg]	90	90	90	90
<i>V</i> [Å ³]	1808.84(16)	4493.19(13)	2707.55(4)	1439.46(2)
<i>Z</i>	4	8	8	4
<i>D</i> _{calcd} (g cm ^{−3})	1.680	1.603	1.774	1.807
λ [Å]	0.71073	0.71073	0.71073	0.71073
μ(Mo Kα), cm ^{−1}	1.409	1.263	1.891	1.791
<i>T</i> [K]	173(2)	218(2)	193(2)	218(2)
2θ _{max} [deg]	28.51	28.15	28.16	26.0
measured reflns	3270	10410	11383	5963
indep reflns	2016 (<i>R</i> _{int} = 0.0192)	4585 (<i>R</i> _{int} = 0.0312)	3154 (<i>R</i> _{int} = 0.0256)	2507 (<i>R</i> _{int} = 0.0392)
reflns with <i>I</i> > 2σ(<i>I</i>)	1858	4250	2960	2190
no. params	212	257	140	162
<i>R</i> (<i>F</i>) ^b (<i>I</i> > 2σ(<i>I</i>)), %	2.66	4.78	3.16	4.93
<i>R</i> _w (<i>F</i> ²) ^c (<i>I</i> > 2σ(<i>I</i>)), %	7.20	17.14	12.39	15.68
GOF	1.032	1.478	1.150	1.324
residual electron density	0.822, −0.423	1.075, −1.650	0.428, −2.705	0.758, −0.658

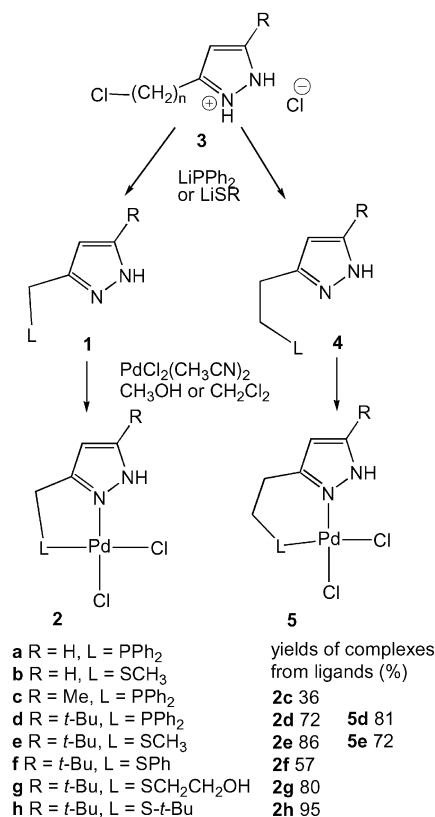
^a Diffractometer used for all compounds was a Bruker Smart Apex CCD. ^b $R = \sum ||F_o| - |F_c|| / \sum |F_o|$. ^c $R_w(F^2) = \{\sum [w(F_o^2 - F_c^2)^2] / \sum [w(F_o^2)^2]\}^{1/2}$; $w = 1/[\sigma^2(F_o^2) + (aP)^2 + bP]$, $P = [2F_c^2 + \max(F_o, 0)]/3$.

Table 2. Collection Data for Crystal Structures of **2h**, **5d**, **5e**^a

	2h	5d	5e
formula	C ₁₂ H ₂₂ Cl ₂ N ₂ PdS	C ₂₁ H ₂₅ Cl ₂ N ₂ PPd	C ₁₀ H ₁₈ Cl ₂ N ₂ PdS
MW	403.68	513.70	375.62
cryst dimensions (mm ³)	0.25 × 0.25 × 0.10	0.50 × 0.20 × 0.20	0.30 × 0.20 × 0.20
cryst syst	monoclinic	monoclinic	monoclinic
space group	<i>P</i> 2 ₁ / <i>c</i>	<i>P</i> 2 ₁ / <i>c</i>	<i>P</i> 2 ₁ / <i>c</i>
<i>a</i> [Å]	12.1700(9)	21.6515(14)	10.6217(19)
<i>b</i> [Å]	22.2275(17)	9.7465(6)	10.7784(19)
<i>c</i> [Å]	12.7895(10)	23.3093(15)	12.812(2)
α [deg]	90	90	90
β [deg]	90.055(1)	117.238(1)	107.328(3)
γ [deg]	90	90	90
<i>V</i> [Å ³]	3459.7(5)	4373.4(5)	1400.2(4)
<i>Z</i>	8	8	4
<i>D</i> _{calcd} (g cm ^{−3})	1.550	1.560	1.782
λ [Å]	0.71073	0.71073	0.71073
μ(Mo Kα), cm ^{−1}	1.489	1.175	1.832
<i>T</i> [K]	153(2)	153(2)	173(2)
2θ _{max} [deg]	28.29	28.28	28.30
measured reflns	40029	49800	6810
indep reflns	8305 (<i>R</i> _{int} = 0.0412)	10495 (<i>R</i> _{int} = 0.0424)	3069 (<i>R</i> _{int} = 0.0336)
reflns with <i>I</i> > 2σ(<i>I</i>)	7328	8613	2461
no. params	326	487	149
<i>R</i> (<i>F</i>) ^b (<i>I</i> > 2σ(<i>I</i>)), %	3.45	4.17	3.09
<i>R</i> _w (<i>F</i> ²) ^c (<i>I</i> > 2σ(<i>I</i>)), %	8.03	8.38	7.24
GOF	1.165	1.095	1.046
residual electron density	0.648, −1.034	0.696, −0.580	0.585, −0.696

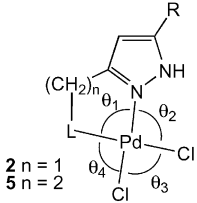
^a Diffractometer used for all compounds was a Bruker Smart Apex CCD. ^b $R = \sum ||F_o| - |F_c|| / \sum |F_o|$. ^c $R_w(F^2) = \{\sum [w(F_o^2 - F_c^2)^2] / \sum [w(F_o^2)^2]\}^{1/2}$; $w = 1/[\sigma^2(F_o^2) + (aP)^2 + bP]$, $P = [2F_c^2 + \max(F_o, 0)]/3$.

construct precursors **3** (Scheme 2) in which substituent *R* can be methyl, *i*-propyl, phenyl, *tert*-butyl, or adamantyl and the side-chain length can be varied.⁶³ Because over 30 g of **3** could be made in four steps in a matter of 2 days in overall

Scheme 2

71% yield, a variety of thioether and phosphine ligands **1** and **4** were readily available using the chemistry shown.

For the purposes of this paper, thioether and phosphine ligands **1** and **4** were used in facile ligand exchange on dichloropalladiumbis(acetonitrile), leading to a total of eight new complexes of type **2** and **5** (Scheme 2). The complexes

Table 3. Main Bond Lengths (Å) and Angles θ (deg) in **2** and **5**


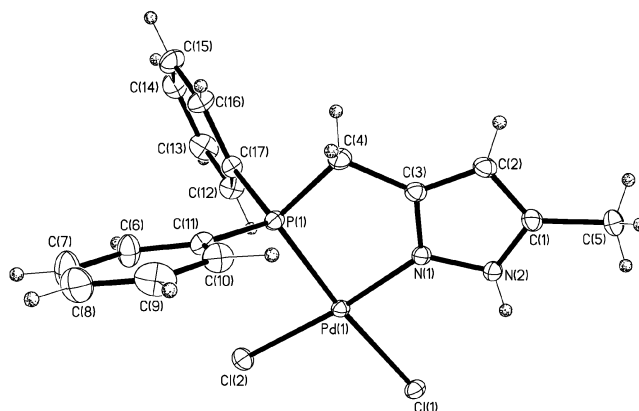
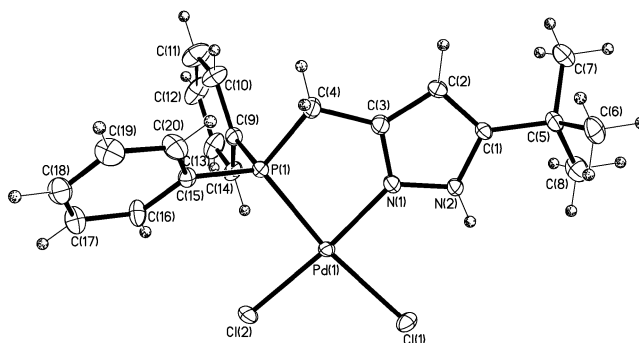
	<i>n</i>	L	R	Pd–Cl trans to L	Pd–Cl trans to N	Pd–L	Pd–N	θ_1	θ_2	θ_3	θ_4
2c	1	Ph ₂ P	Me	2.4719(8)	2.2215(11)	2.2847(9)	1.953(3)	83.23(8)	92.84(8)	95.06(4)	89.04(4)
2d	1	Ph ₂ P	<i>t</i> -Bu	2.3842(11)	2.2944(12)	2.2440(11)	2.014(4)	82.2(1)	89.9(1)	94.7(4)	93.2(4)
2e	1	MeS	<i>t</i> -Bu	2.3477(7)	2.3108(7)	2.2792(7)	2.003(2)	83.64(7)	90.89(7)	95.30(3)	90.08(3)
2g	1	HOCH ₂ CH ₂ S	<i>t</i> -Bu	2.3124(17)	2.7773(18)	2.2487(15)	1.9928(53)	84.72(15)	93.59(15)	93.94(7)	87.75(7)
2h^a	1	<i>t</i> -BuS	<i>t</i> -Bu	2.334(1),	2.295(1),	2.276(1),	1.981(3),	83.6(1),	88.5(1),	95.36(4),	92.52(4),
				2.333(1)	2.298(1)	2.275(1)	1.972(3)	83.4(1)	89.0(1)	95.04(4)	92.59(4)
5d^a	2	Ph ₂ P	<i>t</i> -Bu	2.3891(8),	2.2831(8),	2.2411(8),	2.056(3),	91.11(7),	90.14(7),	90.23(3),	88.54(3),
				2.4005(8)	2.2764(8)	2.2330(8)	2.056(3)	91.27(7)	90.13(7)	90.16(3)	87.93(3)
5e	2	MeS	<i>t</i> -Bu	2.3293(9)	2.274(1)	2.2674(9)	2.010(3)	93.22(8)	89.88(8)	91.54(3)	85.36(3)

^a Two independent molecules in unit cell.

all are air-stable solids and appear to form in high yields, which in some cases (e.g., **2c**) were lowered after crystallization. The *tert*-butyl derivatives in particular displayed good solubility in relatively nonpolar organic solvents such as dichloromethane or chloroform.

The ¹H and ¹³C NMR data for **2** and **5** showed sharp peaks in the expected ranges, in informative contrast to the situation encountered for the ligands. Carbon NMR data for both the ligands and complexes showed three signals for the pyrazole ring carbons in similar ranges, the one for C4 in the range 100–105 ppm and the two for C3 and C5 downfield, between 145 and 158 ppm. However, as noted before,⁶³ ¹³C NMR spectra of **1** and **4** provided evidence of tautomerization, in that the two downfield resonances for C3 and C5, those carbons closest to the shifting proton, were unusually broadened.⁷² (Only one tautomer is shown in the schemes and chart for clarity.) In contrast, with the metal coordinated to the nitrogen shown in **2** and **5**, ¹³C NMR resonances for all pyrazole ring carbons are sharp, and moreover, the N–H proton resonance also is sharper than in proton NMR spectra of the free ligands. We ascribe these changes to the existence of a single tautomer in the complexes, a result supported by X-ray diffraction studies in the solid state.

X-ray Crystal Structures. Seven samples were analyzed at temperatures between 153 and 218 K. Collection data are summarized in Tables 1 and 2, and key bond lengths and angles are shown in Table 3. In the cases of **2h** and **5d**, two

**Figure 1.** Molecular structure of **2c**. Thermal ellipsoids are at 30% probability.**Figure 2.** Molecular structure of **2d**. Thermal ellipsoids are at 30% probability.

independent molecules were seen in the unit cell, so for these complexes Table 3 shows two sets of values. First, general trends in the metrical parameters will be discussed, followed by examples of the changes in hydrogen bonding as a function of ligand. (Figures 1–6 show the molecular structure of representative complexes. For the other species listed in Tables 1–3, see Supporting Information.)

Representative structures are those of **2c** and **2d**, shown in Figures 1 and 2. All complexes feature slightly distorted square-planar geometries. In all cases, the sum of the four angles θ_1 – θ_4 is equal to 360.0°, within experimental

- (65) Schenck, T. G.; Downes, J. M.; Milne, C. R. C.; Mackenzie, P. B.; Boucher, H.; Whelan, J.; Bosnich, B. *Inorg. Chem.* **1985**, *24*, 2334–2337.
- (66) Juanes, O.; de Mendoza, J.; Rodriguez-Ubis, J. *J. Chem. Soc., Chem. Commun.* **1985**, 1765–1766.
- (67) Di Vaira, M.; Mami, F.; Stoppioni, P. *J. Chem. Soc., Dalton Trans.* **1994**, 3739–3743.
- (68) Singh, K.; Long, J. R.; Stavropoulos, P. *Inorg. Chem.* **1998**, *37*, 1073–1079.
- (69) Zadycowicz, J.; Potvin, P. G. *J. Org. Chem.* **1998**, *63*, 235–240.
- (70) Satake, A.; Nakata, T. *J. Am. Chem. Soc.* **1998**, *120*, 10391–10396.
- (71) Ward, M. D.; Fleming, J. S.; Psillakis, E.; Jeffery, J. C.; McCleverty, J. A. *Acta Crystallogr., Sect. C* **1998**, *C54*, 609–612.
- (72) Begtrup, M.; Boyer, G.; Cabildo, P.; Cativiela, C.; Claramunt, R. M.; Elguero, J.; Garcia, J. I.; Toiron, C.; Vedsø, P. *Magn. Res. Chem.* **1993**, *31*, 107–168.

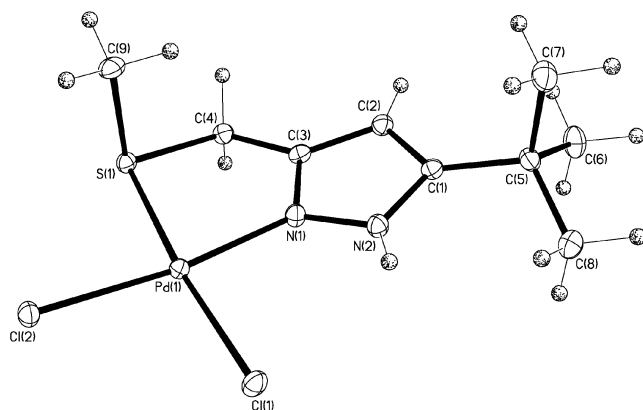


Figure 3. Molecular structure of **2e**. Thermal ellipsoids are at 30% probability.

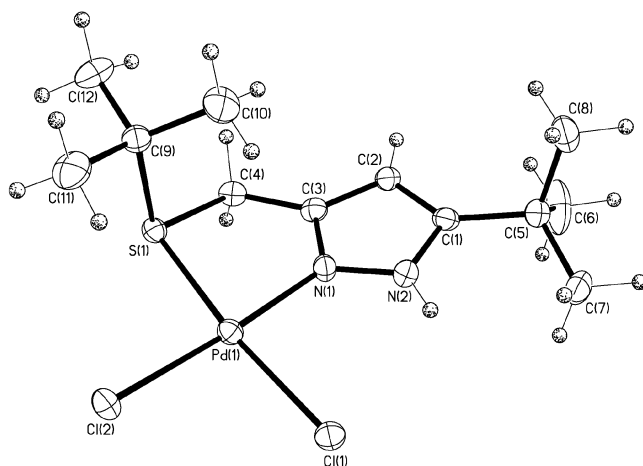


Figure 4. Molecular structure of **2h**. Thermal ellipsoids are at 30% probability.

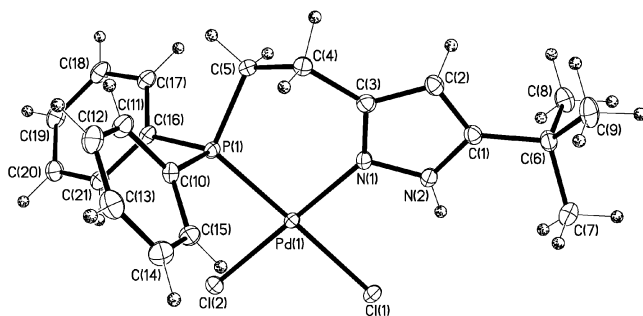


Figure 5. Molecular structure of **2d**. Thermal ellipsoids are at 30% probability.

uncertainty. Palladium–ligand bond lengths are quite constant, even as the size (and steric bulk) of the ligand changes from that of $\text{CH}_3\text{--S--}$ [**2e**, $\text{Pd--S} = 2.279(1)$ Å, Figure 3] to $t\text{-Bu--S--}$ [**2h**, $\text{Pd--S} = 2.276(1)$ or $2.275(1)$ Å, Figure 4]. The greater ground-state trans effect (trans influence) of the phosphine ligand compared with the pyrazole N is shown by the greater lengths of the Pd--Cl bond trans to P compared to those trans to N (differences of 0.090, 0.106 and 0.125, 0.250 Å for **2d**, **5d**, and **2c**, respectively). In the thioether complexes, the Pd--Cl bond trans to S is longer than the one trans to pyrazole N, but the differences are less (in the range 0.037–0.055 Å). Similar differences were seen in previous comparisons of phosphine and thioether complexes.²

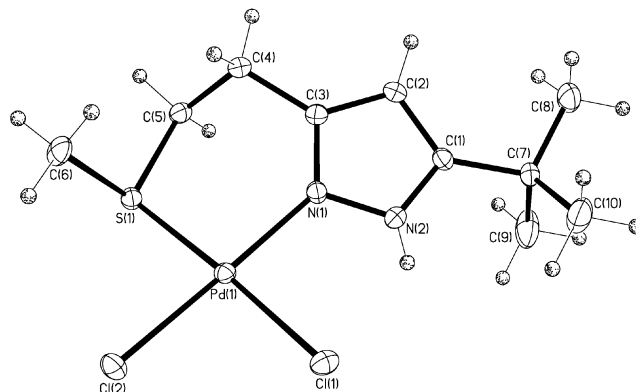


Figure 6. Molecular structure of **2e**. Thermal ellipsoids are at 30% probability.

Table 4. Hydrogen Bonding Contacts in **2** and **5** (Å, deg)

	N(2)–H distance	intramolecular		N(2)–H···Cl(1) angle	intermolecular closest other
		H···Cl(1) distance	N(2)···Cl(1) distance		N(2)–H···Cl contact
2c	0.84(4)	2.71(4)	3.227(4)	121(3)	2.49
2d	0.90(5)	2.58(5)	3.152(4)	122(3)	3.75
2e	0.87(4)	2.67(4)	3.187(3)	119(3)	3.98
2g	0.96(7)	2.69(7)	3.293(6)	121(5)	4.54
2h^a	0.88, 0.88	2.59, 2.60	3.071, 3.077	115, 115	3.77, 3.87
5d^a	0.88, 0.88	2.37, 2.35	2.975, 2.972	127, 128	5.01, 5.02
5e	0.77(3)	2.53(4)	3.040(3)	125(3)	3.78

^a Two independent molecules in unit cell. Positions of pyrazolyl hydrogens not refined.

In four complexes of type **2** where the side chain contains one methylene group, consistent distortions from ideal interligand bond angles of 90° are seen: L--Pd--N and opposing Cl--Pd--Cl angles are smaller [$82.2(1)$ – $84.72(2)^\circ$] and larger [$93.94(7)$ – $95.36(4)^\circ$], respectively, than the ideal values. This difference is reversed in the complexes **5** featuring the longer side chain, where L--Pd--N angles are 0.5 – 1.7° larger than the opposing Cl--Pd--Cl angles.

Hydrogen Bonding. In all complexes examined, the N--H of the coordinated pyrazole appears to participate in a hydrogen bond with the chloride ligand cis to pyrazole. Distances between the hydrogen and the chlorine are in the range $2.35(4)$ – $2.71(4)$ Å, and angles $\text{N}(2)\text{--H}(2)\text{--Cl}(1)$ are in the range 121 – 128° (see Table 4 for intra- and intermolecular contacts). Although these angles are rather small, whereas optimal angles for hydrogen bonding are closer to 180° ,^{73,74} the importance of the hydrogen bonding is suggested by observing the dihedral angle between two planes, that of the pyrazole ring (which includes the N--H) and the square plane defined by Pd and the four ligating atoms. For the complexes with a single methylene group in the side chain, these angles are close to 0° (e.g., for **2c**, it is 2.4°), but this could be because of the rigidity of the five-membered chelate. A better test would be complexes **5d** and **5e** (Figures 5 and 6), which have longer side chains and appear to be more folded. Significantly, here we note that the dihedral angle just defined is still very small (3.8° and 6.8° for the

(73) Pimentel, G. C.; McClellan, A. L. *The Hydrogen Bond*; W. H. Freeman: San Francisco, 1960.

(74) Jeffery, G. A. *An Introduction to Hydrogen Bonding*; Oxford: New York, 1997.

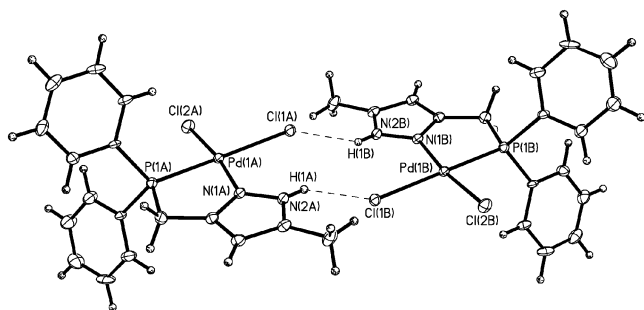


Figure 7. Unit cell packing diagram of **2c**. Thermal ellipsoids are at 25% probability.

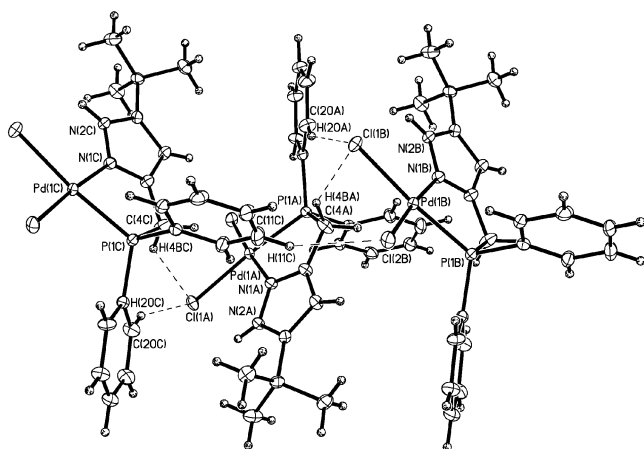


Figure 8. Unit cell packing diagram of **2d**. Thermal ellipsoids are at 25% probability.

two independent molecules of **5d** and 25.6° for **5e**), showing that the N–H vector is close to the square plane of the complex, maximizing intramolecular hydrogen bonding.

The major *difference* between the complexes studied is the number and distances of intermolecular hydrogen bonding interactions. In our previous work on **1**, in fact, the *intermolecular* distance between one N–H and a chloride was less than the intramolecular one.² In this work, the structure of methyl-substituted (diphenylphosphinomethyl)-pyrazole complex **2c** (Figure 1) shows a pairing of molecular units in the unit cell, although the intermolecular distance between Cl(1) and pyrazole N–H(2A) [2.71(4) Å] is somewhat greater than the intramolecular distance Cl(1)–H(2) [2.49(3) Å]. The unit cell packing diagram is shown in Figure 7. In contrast, in *tert*-butyl substituted analogue **2d** (Figure 8), intermolecular contacts between the pyrazole N–H and chloride ligands are absent, the closest such distance being 3.75 Å (see rightmost column of Table 4). The diphenylphosphino group in **2d** is large, but the closest intermolecular N(2)–H···Cl contact of 3.98 Å and the packing diagram of even thioether complex **2e** (Figure 9) show the ability of the pyrazole *tert*-butyl group to block intermolecular hydrogen bonding. In **2e**, the small CH₃S– group allows for intermolecular Pd–S contacts of 3.643(1) Å, distinct from hydrogen bonding. Significantly, the packing diagrams of other *tert*-butyl-substituted derivatives (**2h**, **5d**, **5e**, see Supporting Information) also show the ability of the

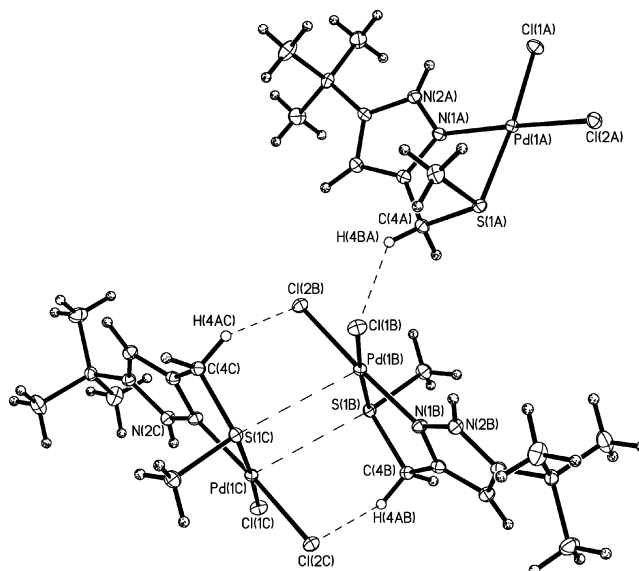


Figure 9. Unit cell packing diagram of **2e**. Thermal ellipsoids are at 25% probability.

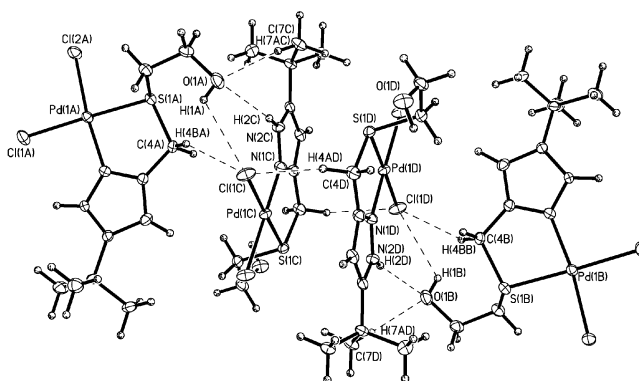


Figure 10. Unit cell packing diagram of **2g**. Thermal ellipsoids are at 25% probability.

large pyrazole substituent to block N(2)–H···Cl closest intermolecular contacts, which range from 3.75 to 5.02 Å (Table 4).

The packing diagram of (2-hydroxyethyl)thioether complex **2g** (Figure 10) is exceptional in the series. Figure 10 shows the ability of the coordinated pyrazole N–H and chloride ligands to enter into hydrogen bonding with the O–H of a neighboring molecule in the crystal. This interaction may model that between water or hydroxylic solvents and the bifunctional pyrazole–chloride complex. The intermolecular contact between the pyrazole H of one molecule and oxygen of another is less [2.33(3) Å] than the intramolecular N–H···Cl contact [2.69(3) Å]. Meanwhile, the hydroxyl H of one molecule is only 2.75 Å distant from the chloride ligand of a neighbor. The intermolecular interactions may play a role in bifunctional activation of substrates.

Solution Studies of Hydrogen Bonding and Acidity. Although solid-phase structural data show evidence of hydrogen bonding, we wished to obtain more evidence for these effects, particularly in solution. In addition, because as far as we are aware, only two papers in the literature give

acidity data for pyrazole complexes,^{59,60} we have used our new complexes to examine solution-phase acidity.

In order to identify unambiguously the N–H stretching frequency in the complexes, an isotopic substitution study was done on **2e**: first, the complex was stirred with CD₃-OD, and the resulting mixture was evaporated. This process was repeated twice more to produce **2e-d**. Dissolution of **2e-d** thus obtained in CH₂Cl₂ (5 mg/mL) gave a solution whose IR spectrum showed a strong absorption at 2498 cm⁻¹ and a weaker one at 3342 cm⁻¹.⁷⁵ No other differences between the spectra of **2e** and its deuterated analogue were noted, and only the absorption at 3342 cm⁻¹ was exhibited by **2e** itself. Considering the reduced masses of the N–H and N–D bonds, for $\nu_{\text{NH}}/\nu_{\text{ND}}$ a ratio of 1.369 is predicted, compared with the ratio of 1.337 observed. In conclusion, we assign the absorption at 3342 cm⁻¹ to the pyrazole N–H stretching frequency. A similar solution of related phosphine complex **2d**, which was also soluble in CH₂Cl₂, showed $\nu_{\text{NH}} = 3312$ cm⁻¹.⁷⁶

Of particular interest would be comparison of hydrogen bonding behavior of **2b** and *tert*-butyl-substituted analogues such as **2e** and **5e**. Unfortunately, **2b** was totally insoluble in CH₂Cl₂, but in the more polar CH₃CN, it was soluble only to the extent of about 1 mg/mL (ca. 0.002 M). Under these conditions, a somewhat broad peak ascribed to the N–H was seen centered at about 3325 cm⁻¹. Better signal-to-noise was achieved in spectra of **2e** in CH₃CN, which showed a peak at 3339 cm⁻¹. It would have been of interest to examine the IR spectra of **2b** as a function of concentration, but its extremely poor solubility characteristics precluded such a study. Our tentative conclusion is that the very similar IR characteristics of **2b** and **2e** in CH₃CN solution suggest that both species are monomeric, at least at concentrations near 0.002 M.

The acidity of complexes **2e** and **5e** was studied by a combination of NMR, IR, and mass spectroscopies in CD₃-CN because it was felt that such a polar solvent gave the best chance of keeping even ionic species in solution, while maintaining the ability to dissolve the neutral starting materials. Neither complex **2e** nor **5e** reacted to a detectable extent (<5%) with equimolar amounts of pyridine or 2,6-lutidine, putting an upper limit on their acidity, because the pK_a of pyridinium ion in CH₃CN is reported to be 12.33.⁷⁷ However, after addition of 100 equiv of pyridine, precipitation occurred. A similar precipitation occurred when only 1 equiv of the stronger base triethylamine (pK_a in CH₃CN =

18.46⁷⁷) was added. When 2 equiv of *N*-methylimidazole (whose basicity in acetonitrile is unknown) was employed, no precipitate was seen, yet the NMR spectrum of the solution had changed to show the appearance of some of the corresponding free pyrazole ligand. Analysis of the various precipitates and the supernatant solutions by direct-injection electrospray mass spectrometry showed only the presence of Pd-containing species containing two Pd atoms and pyrazole ligands and one to three chlorides, suggesting that deprotonation leads to dimeric structures related to **E** (cf. ref 62), whose precise structures must remain the subject of future reports. Regardless, from mass spectrometry data it appears that determination of the acidities of coordinated pyrazoles is made more difficult by the ability of the pyrazolate ligand to form bridging species, a difficulty well-documented in the case of the metal aquo ion of Pd(II).⁷⁸

In summary, we find that, in acetonitrile, pyrazole ligands in Pd(II) complexes exhibit pK_a values between 12.4 and 18.5, probably closer to the former value. Because the pK_a values of a variety of amines are from 6 to 8 units higher in acetonitrile than in water,⁷⁷ we estimate further that should pyrazole–Pd(II) complexes be dissolved in neutral aqueous solutions, they could show pK_a values near 7, considerably lower than the pK_a of free pyrazole (14.2).⁶¹

Conclusions

The ability of pyrazole to donate a hydrogen bond has been explored using a series of new ligands featuring two ring substituents. The substituent at C3 with a short side chain and a ligating thioether or phosphine group L (–CH₂L or –CH₂CH₂L) is designed to anchor a metal firmly to the pyrazole, by forming a chelate between L and the ring nitrogen closest to the side chain. Several Pd(II) complexes of this type were made and characterized by X-ray diffraction, to show the nature of hydrogen bonding between pyrazole N–H and chloride ligands. The second substituent at C5 can be methyl, *i*-propyl, *tert*-butyl, 1-adamantyl, or phenyl, and the identity of this group clearly influences the accessibility of the pyrazole NH for hydrogen bonding. Attempts to corroborate these results using IR spectroscopy were thwarted by great differences in solubility behavior, but solution studies using three organic bases in acetonitrile suggested the degree of acidification of the coordinated pyrazole. Future papers will explore these effects and the acidity and basicity of pyrazole and pyrazolate ligands in a variety of contexts.

Acknowledgment. San Diego State University is thanked for their support of the preparative work. NSF funded the electrospray mass spectrometer (CHE-0116758) and the 500 MHz NMR spectrometer (CHE-9413802) used at SDSU.

Supporting Information Available: Figures showing molecular structure of **2g** and unit cell packing diagrams of **2h**, **5d**, and **5e**, and the CIF file for all seven structures reported in this paper. This material is available free of charge via the Internet at <http://pubs.acs.org>.

IC026104N

(75) We presume that traces of undeuterated material remaining came from partial substitution or exchange with traces of water in the IR cell.

(76) A comparison of this value with those found for the free ligands,⁶³ which all have one relatively small –CH₂L substituent at position 3 on the ring, probably cannot shed light on the question of hydrogen bonding in the complexes, because of the known ability of even 3,5-dimethylpyrazole to form oligomers through hydrogen bond networks: Smith, J. A. S.; Wehrle, B.; Aguilar-Parrilla, F.; Limbach, H. H.; Foces-Foces, M. de la C.; Cano, F. H.; Elguero, J.; Baldy, A.; Pierrot, M.; Khurshid, M. M. T.; Lacombe-Douall, J. B. *J. Am. Chem. Soc.* **1989**, *111*, 7304–7312.

(77) Coetzee, J. F.; Padmanabhan, G. R. *J. Am. Chem. Soc.* **1965**, *87*, 5005–5010.

(78) Shi, T.; Elding, L. I. *Acta Chem. Scand.* **1998**, *52*, 897–902.